

The Radio Wavelength Time Delay of Gravitational Lens 0957+561

D. B. Haarsma^{1,2}, J. N. Hewitt², J. Lehar³, and B. F. Burke²

ABSTRACT

The gravitational lens 0957+561 was monitored with the Very Large Array from 1979 to 1997. The 6 cm light curve data from 1995-1997 and the 4 cm data from 1990-1997 are reported here. At 4 cm, the intrinsic source variations occur earlier and are twice as large as the corresponding variations at 6 cm. The VLBI core and jet components have different magnification factors, leading to different flux ratios for the varying and non-varying portions of the VLA light curves. Using both the PRHQ and Dispersion statistical techniques, we determined the time delay, core flux ratio, and excess non-varying B image flux density. The fits were performed for the 4 cm and 6 cm light curves, both individually and jointly, and we used Gaussian Monte Carlo data to estimate 68% statistical confidence levels. The delay estimates from each individual wavelength were inconsistent given the formal uncertainties, suggesting that there are unmodeled systematic errors in the analysis. We roughly estimate the systematic uncertainty in the joint result from the difference between the 6 cm and 4 cm results, giving 409 ± 30 days for the PRHQ statistic and 397 ± 20 days for the Dispersion statistic. These results are consistent with the current optical time delay of 417 ± 3 days, reconciling the long-standing difference between the optical and radio light curves and between different statistical analyses. The unmodeled systematic effects may also corrupt light curves for other lenses, and we caution that multiple events at multiple wavelengths may be necessary to determine an accurate delay in any lens system. Now that consensus has been reached regarding the time delay in the 0957+561 system, the most pressing issue remaining for determining H_0 is a full understanding of the mass distribution in the lens.

Subject headings: distance scale – gravitational lensing — quasars: individual (0957+561)

¹Haverford College, Haverford, PA 19041, dhaarsma@haverford.edu

²Department of Physics, 37-607, Massachusetts Institute of Technology, Cambridge, MA 02139

³Harvard-Smithsonian Center for Astrophysics, 60 Garden Street, Cambridge, MA 02138

1. Introduction

The time delay between multiple gravitationally lensed images can be used to measure the distance of high redshift objects, and thus is a useful estimator of the Hubble parameter, H_0 . After many years of monitoring the lens 0957+561, the time delay estimates for this system are finally converging on an accepted value. Groups monitoring 0957+561 at optical wavelengths have detected a sharp variation in each image, and have found the optical delay to be 417 ± 3 days (Kundić *et al.* 1995, 1997; Oscoz *et al.* 1997; Schild & Thomson 1997). Given the long controversy over the value of the delay (for a history, see Table 1 of Haarsma *et al.* 1997, hereafter Paper 1), it is important that the optical measurement be confirmed at radio wavelengths. The MIT radio astronomy group has monitored the source at radio wavelengths from 1979 to 1997 and the final light curve data and time delay results are reported here.

2. Observations

Observations have occurred monthly at the National Radio Astronomy Observatory (NRAO) Very Large Array radio telescope (VLA)⁴ since 1979 at 6 cm and since 1990 at 4 cm. The monitoring ended in December 1997. All of the data were reduced in the manner described in Paper 1 and Lehár *et al.* (1992). To determine the flux densities of the point images, it was necessary to subtract the extended structure in the field. At both 6 and 4 cm, this subtraction was difficult in the most compact VLA array, D, thus there are gaps in the light curves for 4 months of every 16 month cycle. In addition, some observations in other VLA arrays were excluded due to bad weather or poor subtraction of the extended structure. When the observations were made in a combination or non-standard array configuration, the data were analyzed according to the next largest standard configuration (A, B, or C).

The 6 cm data through December 1994 were presented in Paper 1. The remaining 6 cm data and all of the 4 cm data are given in Tables 1 and 2, and plotted in Figure 1. The light curve data are also available electronically through <http://space.mit.edu/RADIO/papers.html>. There are a total of 147 points in the 6 cm light curve, and 58 points in the 4 cm light curve. At 6 cm, the flux density of the B image increased in 1995, following the A image increase in 1994. The current 6 cm feature has

⁴The National Radio Astronomy Observatory is operated by Associated Universities, Inc., under cooperative agreement with the National Science Foundation.

lasted longer than the similar feature around 1989-1991, but the A image is now declining. At 4 cm, the quasar is twice as variable as at 6 cm (as a percentage of average flux density). Also, the variations in the 4 cm light curves occur earlier than the corresponding features at 6 cm. Both of these characteristics are consistent with multi-wavelength models and other observations of AGN variability (*e.g.* Marscher & Gear 1985; Stevens *et al.* 1996). The well-sampled increase and decrease at 4 cm in 1994-97 has helped significantly in determining the radio time delay.

3. Free parameters in the Light Curves

When fitting for the time delay between the images, the difference in magnification between them must be properly taken into account. In past analyses of lensed light curves (including Paper 1), only two parameters were used in the fit: the time delay and a single flux ratio. Conner, Lehár, & Burke (1992), however, have pointed out that the magnification varies rapidly along the B image, causing the VLBI core and jet components to have different flux ratios, with the core ratio being larger. At the resolution of the VLA, the beam includes both the core and the jet, and thus the flux ratio of the VLA light curves R_{VLA} is a composite of the core and jet values. The VLA light curve is the sum of the jet (which is constant in time), and the core (which has both variable and constant components). There are then four physical parameters: the time delay τ , the flux ratio of the core $R_{\text{core}} = B_{\text{core}}/A_{\text{core}}$, the flux ratio of the jet $R_{\text{jet}} = B_{\text{jet}}/A_{\text{jet}}$, and the amount of flux density due to the jet vs. the core, *i.e.* $B(t) = B_{\text{core}}(t) + B_{\text{jet}}$ for the B image. Note that the core can contain both constant (DC) and variable (AC) components, *i.e.* $B_{\text{core}} = B_{\text{core,DC}} + B_{\text{AC}}$. Also, the DC part of the light curve is due to both the core and the jet, *i.e.* $B_{\text{DC}} = B_{\text{core,DC}} + B_{\text{jet}}$.

Press & Rybicki (1998) discuss these issues in the context of the optical light curves of 0957+561. They point out that the amount of constant flux due to the core ($B_{\text{core,DC}}$) is impossible to determine, since we may have not yet seen the variable part of the core (B_{AC}) go to zero. They show that on a fundamental level there are only three measureable parameters in a pair of lensed light curves, which may be cast as: the time delay τ , the core flux ratio R_{core} , and the extra constant flux in the B image that does not occur in the A image,

$$c = \frac{B_{\text{DC}}}{R_{\text{AC}}} - A_{\text{DC}} \quad (1)$$

(Press & Rybicki 1998), where R_{AC} is the flux ratio of the variable component. It is useful

to write c in terms of the core and jet components of the radio images as

$$c = \frac{B_{\text{jet}} + B_{\text{core,DC}}}{R_{\text{core}}} - (A_{\text{jet}} + A_{\text{core,DC}}), \quad (2)$$

and therefore

$$c = B_{\text{jet}} \left(\frac{1}{R_{\text{core}}} - \frac{1}{R_{\text{jet}}} \right), \quad (3)$$

where the DC core components cancel out. The value of c can thus be estimated from the values of B_{jet} , R_{core} , and R_{jet} . Since in the case of 0957+561 we have $R_{\text{jet}} < R_{\text{core}}$ (Conner, Lehár, & Burke 1992), the value of c must be negative; *i.e.* the A curve has a larger amount of constant flux than the core-ratio corrected B curve.

The values of several of the above parameters can be estimated from observations without doing time delay fitting. Garrett *et al.* (1994) compiled the information on the core flux ratio from VLBI and optical observations, and found the weighted average of these estimates to be $R_{\text{core}} = 0.75 \pm 0.02$. Also, the faintest portions of the VLA light curves set upper limits on the jet flux density, *i.e.* $B_{\text{jet}} \lesssim 21$ mJy at 6 cm, and $B_{\text{jet}} \lesssim 15$ mJy at 4 cm. A better estimate of B_{jet} can be obtained by comparing coincident VLBI and VLA observations. The VLBI observations give the core flux density at a particular epoch, which can be subtracted from the VLA flux density to obtain the VLA jet flux density. Campbell *et al.* (1995) report VLBI observations at 6 cm on 1987 Sep 28 and 1989 Sep 26, and by comparing these to VLA observations occurring on the same days we find $B_{\text{jet}} = 11.1 \pm 0.4$ mJy and $R_{\text{jet}} = 0.63 \pm 0.03$. The values for R_{core} , R_{jet} , and B_{core} can be combined using equation 3 to find $c_6 = -2.7 \pm 0.8$ mJy.

The above estimates are all for the 6 cm light curves. At 4 cm there are no coincident VLBI/VLA observations, so we can not make similar estimates. The value of c is different at 6 cm and 4 cm due to the difference in B_{jet} ; note that the ratios R_{jet} and R_{core} are the same for the two bands. For a synchrotron spectrum, B_{jet} will be smaller at 6 cm than 4 cm, and thus we expect $|c_4|$ to be smaller than $|c_6|$.

4. Time Delay Analysis Methods

To fit for the three parameters τ , R_{core} , and c (described in §3), we used the PRHQ statistic (Press, Rybicki, & Hewitt 1992a, 1992b; Rybicki & Press 1992; incorporating the modifications of Rybicki & Kleyna 1994; Press & Rybicki 1998), and the Dispersion statistic (Pelt *et al.* 1994, 1996), which were described in Paper 1. We used linear units (mJy) rather than the logarithmic units defined in Paper 1. The discrete correlation function (Lehár *et al.* 1992) did not find a strong correlation in the 4 cm light curves, so that statistic was not

used here. Gaussian Monte Carlo data were made as described in Paper 1, but now with the four physical parameters τ , R_{core} , R_{jet} , and B_{jet} . Five hundred Gaussian Monte Carlo data sets were used to estimate the 68% confidence intervals on the results for the real light curves, where the fitted c values were compared to the input parameters using equation 3. The pseudo-jackknife test from Paper 1 was used to test the stability of the result to the removal of individual points.

To determine whether neglecting the difference between the core and jet flux ratio caused an error in our previous analysis, we applied the two dimensional fit (for τ and R_{VLA} , as in Paper 1) to the Gaussian Monte Carlo data made with four parameters. The resulting fitted-minus-true values did not show a significant bias (to long or short delays, for example), but did show an increase in scatter about the true delay. We found that the error in the delay increased monotonically with B_{jet} , from roughly 20 days for $B_{\text{jet}} = 0$ mJy to roughly 100 days for $B_{\text{jet}} \sim 11$ mJy (the value for the real light curves) when using the PRHQ statistic and the 6 cm Monte Carlo data. The same test with the 4 cm Monte Carlo data, and with the Dispersion statistic at both 4 cm and 6 cm, revealed a similar but somewhat milder effect, with the delay error at least doubling between small and large values of B_{jet} . This dependence on the amount of flux density in the jet component may be one cause of the inconsistency in delay estimates over the years, and we caution that fitting for only two parameters may introduce significant errors.

In addition to analyzing the two wavelengths individually, we also fitted for the parameters using both wavelengths at once. The Dispersion and PRHQ statistics are both easily modified for this by minimizing the sum of the statistics from each wavelength (see Press *et al.* 1992b), and fitting for the parameters τ , R_{core} , c_6 , and c_4 . Monte Carlo analysis was also done for the joint data, where the 6 cm and 4 cm Monte Carlo sets were constructed with the same set of $[\tau, R_{\text{core}}, R_{\text{jet}}, B_{\text{jet}}]$.

The covariance model (Paper 1; Press *et al.* 1992a) used for the PRHQ statistic was found by an iterative procedure on the individual light curves. First, measurement errors of 2% were assumed and used to make point estimates for the structure function, and then fitted to an exponential in the lag range of 100 to 700 days. This structure function was then used to determine the $\text{PRH}\chi^2$ value for the light curve, and the measurement errors were adjusted until $\text{PRH}\chi^2$ equaled the degrees of freedom. Then the process was repeated for the new measurement error value. Iterations stopped when the square root of ($\text{PRH}\chi^2/\text{degrees of freedom}$) changed by less than 1% when $\text{PRH}\chi^2$ was calculated with the measurement error of the previous iteration. At 6 cm, the covariance model found was

$$V(T) = 1.673 \times 10^{-4} T^{1.606} \text{ mJy}^2, \quad (4)$$

with measurement errors $e_A = 1.82\%$ and $e_B = 2.34\%$, where T is the time lag between two

points on the curve. At 4 cm, the fitted covariance model was

$$V(T) = 3.174 \times 10^{-4} T^{1.633} \text{ mJy}^2, \quad (5)$$

with measurement errors $e_A = 1.67\%$ and $e_B = 2.19\%$.

The sharp feature in the B image at 6 cm in Spring 1990 is statistically inconsistent with the rest of the light curve (see Paper 1), and, given the short delay found from the optical and 4 cm light curves, the A image shows that the feature is not intrinsic to the source. Thus we expect that the results with the points removed will be more accurate than the results for the full 6 cm curves. The 6 cm analysis was done both with and without the four points (1990 March 15, April 10, May 7, and May 23); the light curve without the points will be denoted 6*cm.

5. Results

The main results of the time delay analysis are shown in Tables 3 and 4. These and other aspects of the results are worth discussion in this section. First, the Monte Carlo analysis showed that the use of the three parameter fit (τ , R_{core} , c) made the time delay confidence interval independent of B_{jet} (rather than increase with B_{jet} as happened in the two parameter fit described in §4). Next, the pseudo-jackknife test (see Paper 1), using either the PRHQ or Dispersion statistic, showed that removal of an individual point from the light curve general caused a change in the delay that was much smaller than the confidence interval, with a few important points in the curve (typically during rises or falls) causing a change at about the amount of the confidence interval. Thus, the delay estimate in all cases is stable under the removal of individual points. Note also that the removal of the four Spring 1990 points (6*cm vs. 6 cm in Tables 3 and 4) never caused a change in the fitted parameters of more than the confidence interval.

The relationship between the values of c and R_{core} for a given delay is worth pointing out. Figure 2 shows the PRH χ^2 statistic as a function of c and R_{core} for the 6*cm light curves, with the delay fixed at the best fit value. The surface is a diagonal trough, with the location of the minimum poorly constrained along the bottom of the trough. The trend is such that a larger value of R_{core} requires a more negative value of c , as expected from equation 3. The 4 cm light curve has a similar PRH χ^2 surface, and the Dispersion surface shows a similar but even more pronounced effect. Thus, if either R_{core} or c is poorly constrained by the light curves, the other parameter will also be poorly determined.

There is a significant bias in c and R_{core} for the Dispersion statistic, which is related to the interdependence of these parameters. The fitted-minus-true values from the Dispersion

analysis of the Gaussian Monte Carlo data showed a pronounced asymmetry and bias in both c and R_{core} (but was nearly symmetric and un-biased in delay). Tests showed that the bias in c and R_{core} was somewhat reduced for $\delta \sim 25$ days (where δ is a weighting parameter in the Dispersion statistic, see Paper 1). We continued to use $\delta = 60$ days (as done by Pelt *et al.* 1996), since that value had the narrowest distribution for the fitted-minus-true delays. Thus, only the time delay results are given in Table 4.

The PRHQ statistic produced a symmetric distribution in c and R_{core} , and the results are listed in Table 3. Note that the fitted value of c is more negative when R_{core} is larger, as mentioned above. The analysis of the individual wavelengths found somewhat different values of R_{core} , and that c_4 is more negative than c_6 contrary to the predictions of §3. The joint analysis of the two wavelengths, however, used all of the available information to constrain the fit, and the resulting R_{core} , c_6 , and c_4 are in good agreement with the predictions of §3.

Turning now to the results for the delay, it is of interest that all of the delay estimates in Tables 3 and 4 are much smaller than the value of 540 days found by Press *et al.* (1992b) using the first 80 points in the 6 cm light curve. As explained in Paper 1, this change in the delay estimate is due entirely to the addition of new features to the light curve. If the first 80 points in the curve (with or without the four Spring 1990 points) are fitted for the three parameters, the Dispersion statistic finds a delay of roughly 550 ± 35 days, and the PRHQ statistic (using the above covariance model, eq. 4) finds a delay of roughly 525 ± 25 days (the confidence intervals were estimated from Monte Carlo analysis of 100 light curves). Therefore the change in the delay estimate between the first 80 points and the current 147 points occurs for both statistical methods, for fits with two or three parameters, and for a variety of covariance models. It does not, however, occur in our Gaussian Monte Carlo data. Comparing delay estimates from the first 80 points and the full curves in the Monte Carlo data, we find that 99% of the sets have a difference in delay less than the 75 day difference seen in the real light curves. Thus the Monte Carlo light curves must still be missing some characteristic of the real data.

A related issue is the difference in the delay estimates for the two wavelengths (for PRHQ, $\tau_6 = 452_{-15}^{+14}$ days vs. $\tau_4 = 397 \pm 12$ days, a difference of about three confidence intervals). The time delay between lensed images should be completely independent of wavelength, and indeed the optical and radio estimates come remarkably close. This effect also does not occur in the Gaussian Monte Carlo data, which were constructed such that the 6 and 4 cm data have the same set of $[\tau, R_{\text{core}}, R_{\text{jet}}, B_{\text{jet}}]$. When applying the PRHQ statistic, we found that 99% of the Monte Carlo curves had a difference of $(|\tau_6 - \tau_4|)$ that was smaller than the 55 day difference in the real data; similarly, the Dispersion statistic

found that about 80% of the data sets had a smaller delay difference.

Since both of these effects (the significant change in the delay estimate as features are added to the curves, and the significant difference between the two radio wavelengths) are not seen in the Monte Carlo data, there must still be some systematic effect that has not been taken into account in the creation of the Monte Carlo data or in our analysis. One source of the systematic error may be interstellar scintillation, which can cause variability at a level not much larger than our observational error of 2%, perhaps creating small features such as the discrepancy between the 6 cm A and B images in early 1985 (see Figure 4). Although individual features of a few percent are difficult to identify, they may cause a significant bias in the delay estimate if they occur at crucial times in the light curves. We note that microlensing could cause similar low level systematic effects in the optical light curves (Schild & Smith 1991; Schmidt & Wambsganss 1998). Since it is beyond the scope of this paper to model these systematic effects, we make a rough estimate from the difference between the 6 and 4 cm delay estimates, giving a systematic uncertainty of roughly ± 30 days for PRHQ and ± 20 days for the Dispersion. Note that this uncertainty is still less than 10%, and is only one factor contributing to the error in H_0 (see §6). Note also that the optical time delay estimate has a smaller error (only 1%, Kundić *et al.* 1997) primarily because the source varies much more rapidly at optical wavelengths than radio wavelengths. We caution others monitoring gravitational lenses that in order to determine an accurate time delay it is preferable to have light curves with multiple features at multiple wavelengths, since the estimate of the time delay based on a single feature at a single wavelength could easily be corrupted by these low level systematic effects (as the 0957+561 6 cm curves were after the first 80 observations). The 0957 radio light curves will continue to be a useful data set for studying systematic effects and time delay analysis techniques.

Figure 3 shows the PRHQ and Dispersion statistics as a function of delay for the joint analysis of the 4 cm and 6*cm curves, with the values of c_6 , c_4 , and R_{core} fixed at the best fit values. Figure 4 shows the aligned light curves at the two wavelengths with the PRH optimal reconstruction (see Press *et al.* 1992a and Paper 1).

6. Conclusions

Since our last report (Paper 1), the B image has increased at 6 cm, and the A image has entered a slow decline. The 4 cm curves, given here for the first time, are highly variable and give additional features to aid in determining the time delay. To take into account the difference in magnification of the core and jet components of each image, we have fit for the delay, core flux ratio, and the excess flux density in the B image (as defined by Press

& Rybicki 1998). The delay estimates found from the wavelengths individually disagree by a few confidence intervals, indicating that there are systematic effects not modeled in our analysis. The delay estimates found from the joint analyses of both wavelengths were 409 ± 30 days for PRHQ and 395 ± 20 days for the Dispersion, where the uncertainty is based on a rough estimate of the systematic error. Both results are consistent with the delay estimated from optical monitoring (417 ± 3 days, Kundić *et al.* 1997), and thus we now have good agreement for the value of the delay from both statistics in both the radio and optical light curves. Consensus has finally been reached on the value of the delay for gravitational lens 0957+561.

This measurement of the delay can now be used to answer cosmological questions. The Hubble parameter, however, depends not only on the delay but also on the lens model and the galaxy velocity dispersion. Using the SPLS model of Grogin & Narayan (1996a, 1996b), the recent Keck velocity dispersion measurement of 279 km s^{-1} (Falco *et al.* 1997), and a time delay of 409 days, we obtain $H_0=67 \text{ km s}^{-1}\text{Mpc}^{-1}$. In fitting this model, Grogin & Narayan used the ground-based optical position of the lensing galaxy as a constraint, rather than the more precise VLBI position. Since then, the HST optical position of the lensing galaxy has been found to agree with the VLBI position (Bernstein *et al.* 1997). The modelers point out (Grogin & Narayan 1996b) that if the VLBI position is used as the model constraint, their model fit is very similar to that of Falco, Gorenstein, & Shapiro (1991); for the same delay and velocity dispersion, the Falco *et al.* model gives $H_0=41 \text{ km s}^{-1}\text{Mpc}^{-1}$. Thus, the change in the position of the lensing galaxy causes a change in the estimate of H_0 well beyond the statistical error, apparently in contradiction to the conclusions of Kundić *et al.* (1997) regarding the robustness of the H_0 determination. New modeling work must be done which incorporates the improved galaxy position, the recent observations of the cluster mass distribution (Fischer *et al.* 1997), a careful treatment of the systematic errors in the velocity dispersion (Romanowsky & Kochanek 1998), and the recently reported structure at x-ray (Chartas *et al.* 1998), optical (Bernstein *et al.* 1997), and radio (Avruch *et al.* 1997; Harvanek *et al.* 1997) wavelengths. These new observations will allow an improved fit of the model to the data and provide a more accurate measure of the Hubble parameter.

We thank the VLA staff for their assistance over the many years of this monitoring project. DBH and BFB have been supported in part by the National Science Foundation. JNH acknowledges the support of a David and Lucile Packard Fellowship, a NSF Presidential Young Investigator Award, and NSF grant AST 96-17028. JL acknowledges the support of NSF grant AST 93-03527.

REFERENCES

- Avruch, I. M., Cohen, A. S., Lehár, J., Conner, S. R., Haarsma, D. B., & Burke, B. F. 1997, *ApJ*, 488, L121
- Bernstein, G., Fischer, P., Tyson, J. A., & Rhee, G. 1997, *ApJ*, 483, L79
- Campbell, R. M., Lehár, J., Corey, B. E., Shapiro, I. I., & Falco, E. E. 1995, *AJ*, 110, 2566
- Chartas, G., Chuss, D., Forman, W., Jones, C., & Shapiro, I. 1998, preprint astro-ph/9803285
- Conner, S. R., Lehár, J., & Burke, B. F. 1992, *ApJ*, 387, L61
- Falco, E. E., Gorenstein, M. V., & Shapiro, I. I. 1991, *ApJ*, 372, 364
- Falco, E. E., Shapiro, I. I., Moustakas, L. A., & Davis, M. 1997, *ApJ*, 484, 70
- Fischer, P., Bernstein, G., Rhee, G., & Tyson, J. A. 1997, *AJ*, 113, 521
- Garrett, M. A., Calder, R. J., Porcas, R. W., King, L. J., Walsh, D., & Wilkinson, P. N. 1994, *MNRAS*, 270, 457
- Grogin, N. A., & Narayan, R. 1996a, *ApJ*, 464, 92
- Grogin, N. A., & Narayan, R. 1996b, *ApJ*, 473, 570
- Haarsma, D. B., Hewitt, J. N., Lehár, J., & Burke, B. F. 1997, *ApJ*, 479, 102 (Paper 1)
- Harvanek, M., Stocke, J. T., Morse, J. A., & Rhee, G. 1997, *AJ*, 114, 2240
- Kundić, T., *et al.* 1997, *ApJ*, 482, 75
- Kundić, T., Colley, W. N., Gott III, J. R., Malhotra, S., Pen, U.-L., Rhoads, J. E., Stanek, K. Z., & Turner, E. L. 1995, *ApJ*, 455, L5
- Lehár, J., Hewitt, J. N., Roberts, D. H., & Burke, B. F. 1992, *ApJ*, 384, 453
- Marscher, A. P., & Gear, W. K. 1985, *ApJ*, 298, 114
- Oscos, A., Mediavilla, E., Goicoechea, L. J., Serra-Ricart, M., & Buitrago, J. 1997, *ApJ*, 479, L89
- Pelt, J., Hoff, W., Kayser, R., Refsdal, S., & Schramm, T. 1994, *A&A*, 286, 775
- Pelt, J., Kayser, R., Refsdal, S., & Schramm, T. 1996, *A&A*, 305, 97

- Press, W. H., & Rybicki, G. B. 1998, preprint astro-ph/9803193
- Press, W. H., Rybicki, G. B., & Hewitt, J. N. 1992a, ApJ, 385, 404
- Press, W. H., Rybicki, G. B., & Hewitt, J. N. 1992b, ApJ, 385, 416
- Romanowsky, A. J., & Kochanek, C. S. 1998, preprint astro-ph/9805080
- Rybicki, G. B., & Kleyana, J. T. 1994, in Reverberation Mapping of the Broad-Line Region in Active Galactic Nuclei, ed. P. M. Gondhalekar, K. Horne, & B. M. Peterson (San Francisco: Astronomical Society of the Pacific), 85
- Rybicki, G. B., & Press, W. H. 1992, ApJ, 398, 169
- Schild, R., & Thomson, D. J. 1997, AJ, 113, 130
- Schild, R. E., & Smith, R. C. 1991, AJ, 101, 813
- Schmidt, R., & Wambsganss, J. 1998, preprint astro-ph/9804130
- Stevens, J. A., Litchfield, S. J., Robson, E. I., Cawthorne, T. V., Aller, M. F., Aller, H. D., Hughes, P. A., & Wright, M. C. H. 1996, ApJ, 466, 158

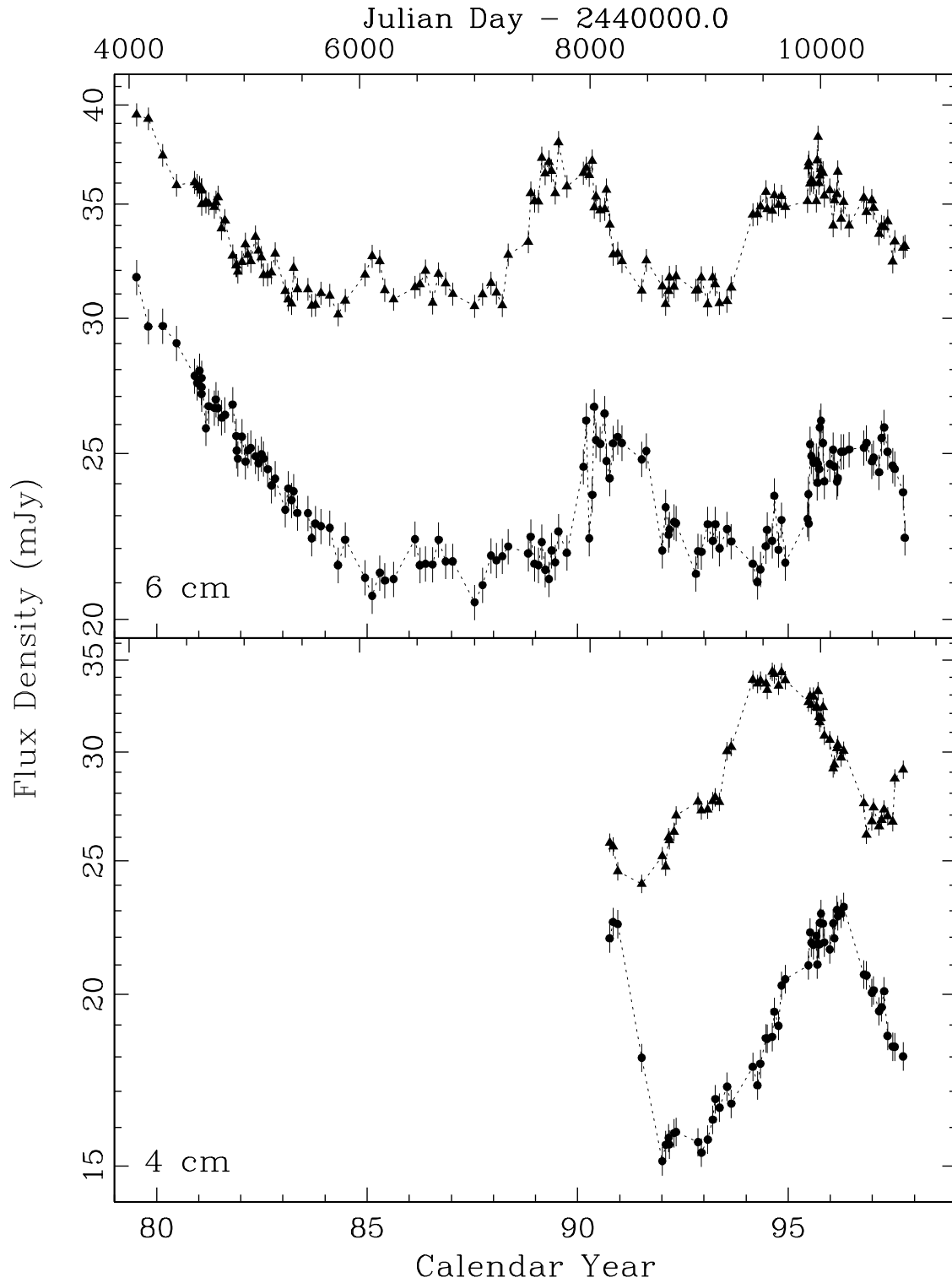


Fig. 1.— The complete 6 cm and 4 cm light curves of gravitational lens 0957+561. The A image data are shown as triangles and the B image as circles. The 4 cm A image has been shifted up by 8% to avoid overlap with the B image.

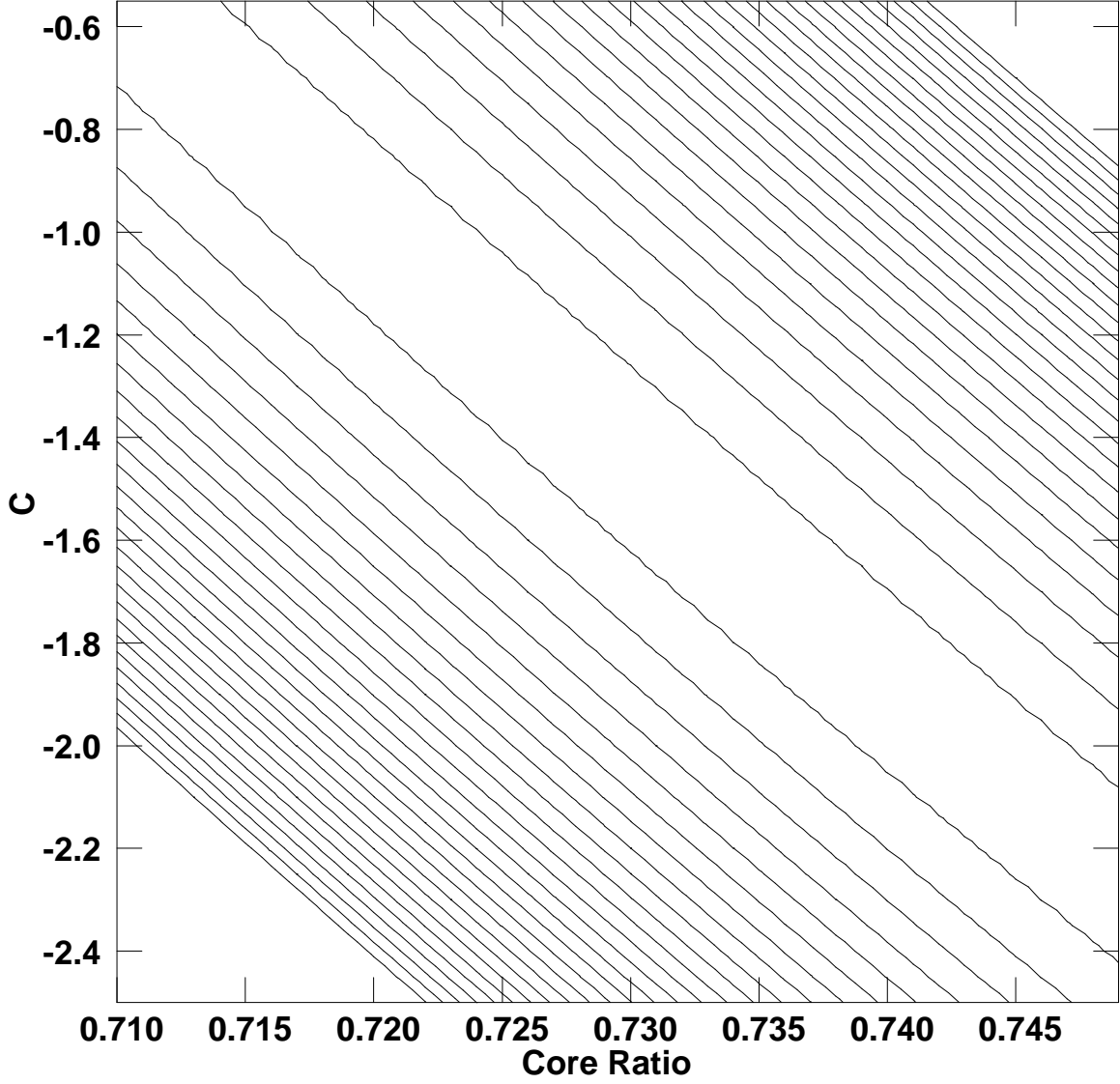


Fig. 2.— PRHQ for the 6*cm light curves, as a function of c and R_{core} . The delay is fixed at 452 days. The minimum is $Q = 125.6$ at $c = -1.47$ and $R_{\text{core}} = 0.731$. Contours start at $Q = 130$ and increase by 10 to $Q = 380$.

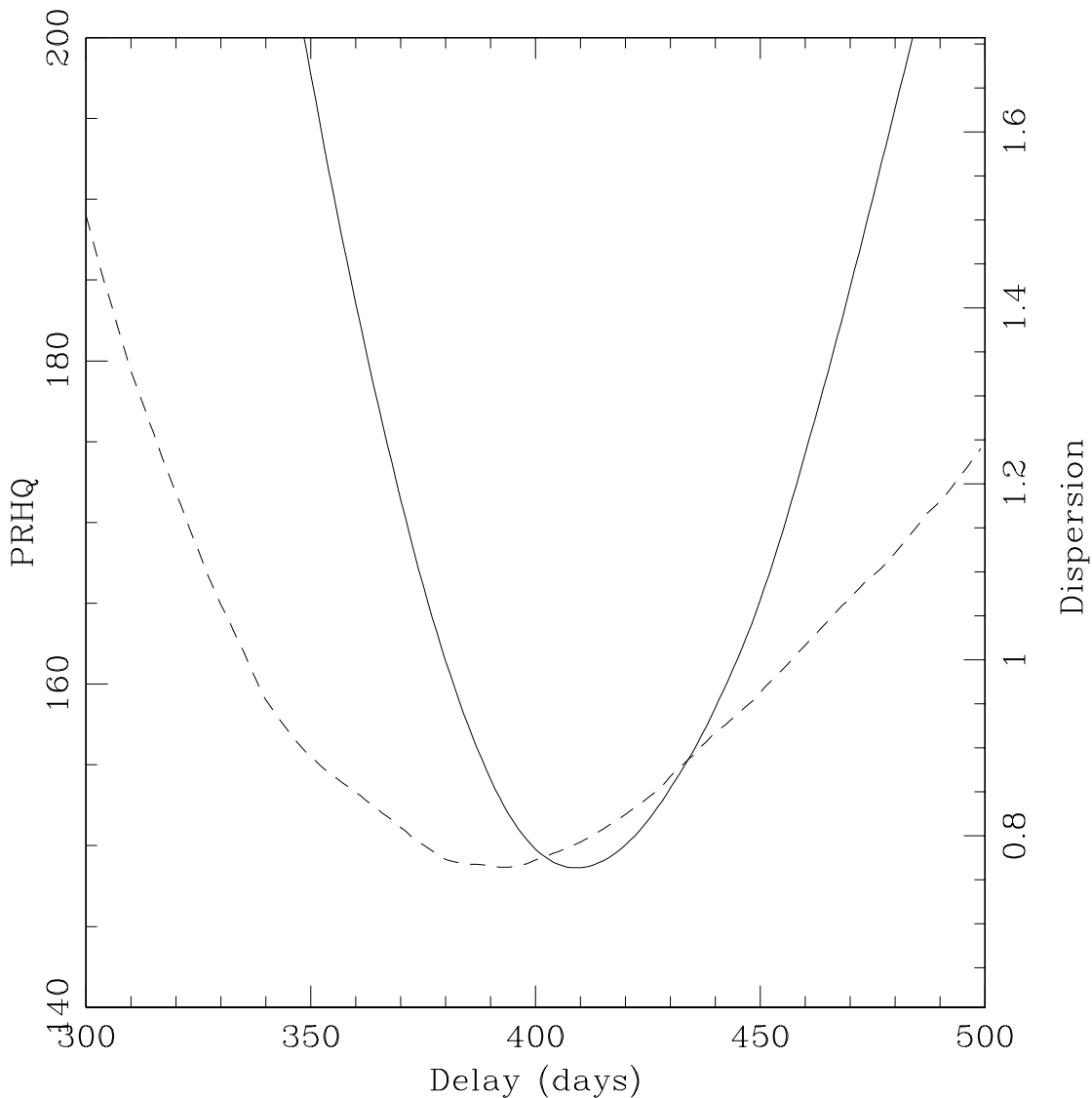


Fig. 3.— Joint time delay analysis of the 6* cm and 4 cm light curves. The PRHQ statistic is shown as a solid line with a minimum at 409 days. The Dispersion statistic is shown as a dashed line with a minimum at 395 days. The values of R_{core} , c_6 , and c_4 were set at the best fit values for purposes of plotting the statistic *vs.* delay. The vertical axes were scaled such that the PRHQ and Dispersion confidence intervals were the same height.

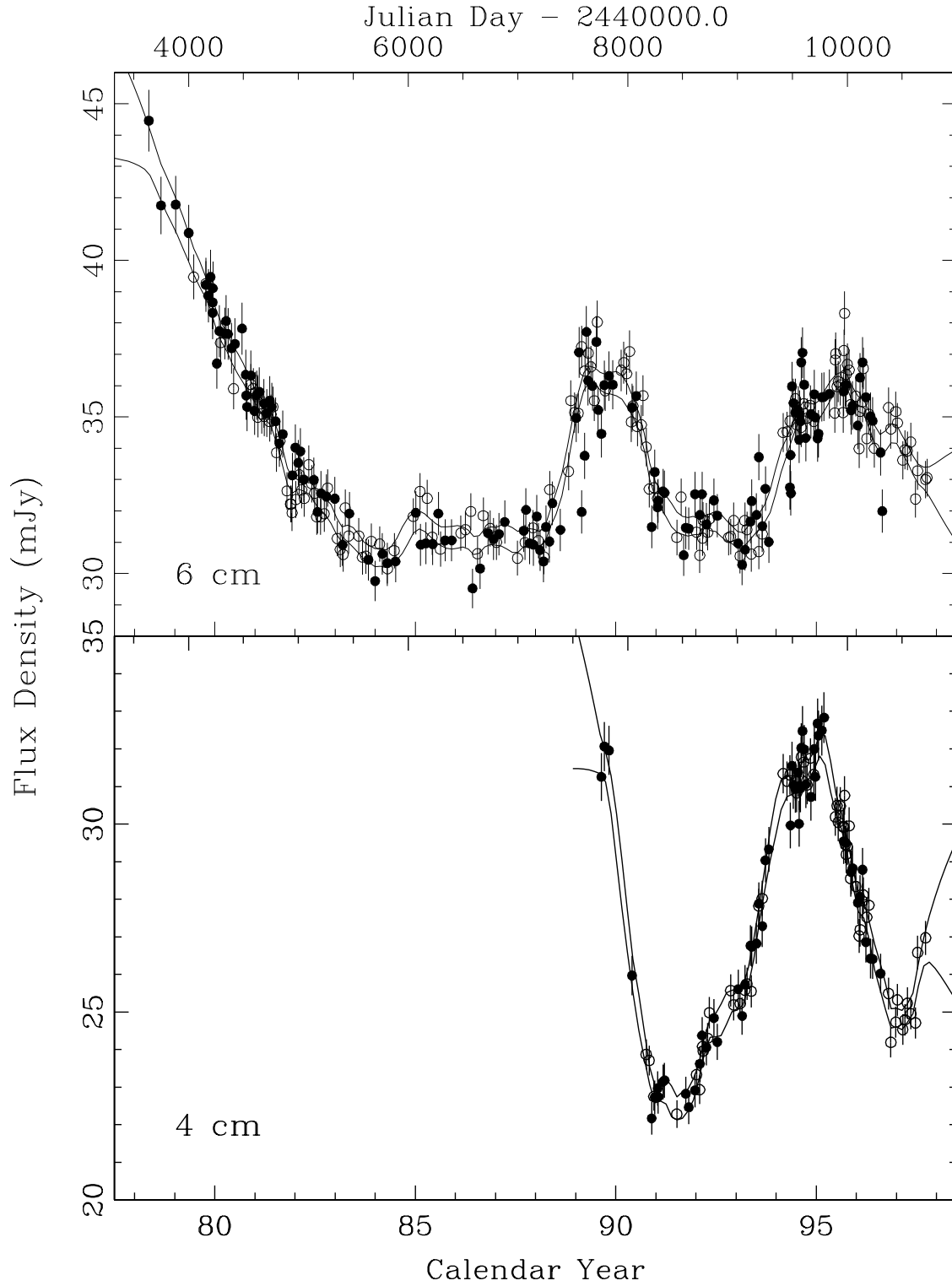


Fig. 4.— The 6 cm and 4 cm light curves combined at $\tau = 409$ days, $R_{\text{core}} = 0.753$, $c_6 = -2.35$, and $c_4 = -2.09$, shifted to the time and flux density of the A image. The A image data are shown as open circles and the B image as solid circles. The one sigma width of the PRH optimal reconstruction is shown as a pair of lines.

Table 1. 6 cm Light Curve Data

Calendar Date	Day ^a	Array	Flux Density (mJy)	
			A Image	B Image
1995 Jun 18	9886.57	D→A	35.13	22.89
1995 Jun 23	9892.50	A	36.82	23.67
1995 Jun 28	9896.53	A	37.02	22.75
1995 Jul 08	9907.23	A	35.97	25.32
1995 Jul 21	9919.51	A	36.13	24.92
1995 Aug 07	9937.34	A	36.02	24.69
1995 Sep 01	9962.33	A	35.14	24.75
1995 Sep 09	9970.14	A→AnB	37.12	24.04
1995 Sep 15	9976.10	AnB	38.31	24.65
1995 Sep 23	9984.17	AnB	35.99	24.48
1995 Sep 30	9991.17	AnB	36.36	25.90
1995 Oct 10	10001.17	B	36.68	26.13
1995 Oct 27	10018.20	B	36.50	25.36
1995 Nov 09	10031.06	B	35.39	24.08
1995 Dec 26	10077.95	B	35.66	24.65
1996 Jan 26	10108.83	BnC	33.99	25.13
1996 Feb 05	10118.77	BnC	35.18	24.57
1996 Feb 26	10139.67	C	35.48	24.07
1996 Mar 04	10146.68	C	36.55	24.18
1996 Apr 05	10178.56	C	34.31	25.06
1996 Apr 25	10198.66	C	35.09	25.07
1996 Jun 11	10246.48	CnD	34.00	25.14
1996 Oct 19	10376.05	A	35.30	25.20
1996 Nov 10	10397.95	A	34.62	25.36
1996 Dec 26	10443.98	A	35.17	24.74
1997 Jan 10	10458.89	A	34.81	24.86
1997 Feb 26	10505.82	B	33.62	24.38
1997 Mar 19	10526.69	B	33.95	25.53
1997 Apr 10	10548.65	B	33.92	25.90
1997 May 11	10579.65	B	34.20	25.06
1997 Jun 22	10622.38	BnC	32.38	24.60
1997 Jul 11	10641.43	C	33.28	24.49
1997 Sep 22	10714.17	C	33.00	23.73
1997 Oct 06	10728.18	CnD	33.06	22.32

Table 1—Continued

Calendar Date	Day ^a	Array	Flux Density (mJy)	
			A Image	B Image

^aJulian Day – 2,440,000.0

Table 2. 4 cm Light Curve Data

Calendar Date	Day ^a	Array	Flux Density (mJy)	
			A Image	B Image
1990 Oct 04	8169.22	BnC	23.87	21.96
1990 Nov 01	8197.06	C	23.71	22.57
1990 Dec 13	8238.89	C	22.75	22.49
1991 Jul 10	8448.40	A	22.28	17.98
1992 Jan 06	8627.97	B	23.33	15.12
1992 Feb 04	8656.80	BnC	22.93	15.54
1992 Feb 29	8681.74	C	24.08	15.72
1992 Mar 07	8688.67	C	23.96	15.55
1992 Apr 18	8730.60	C	24.30	15.85
1992 May 03	8745.60	C	24.98	15.88
1992 Nov 11	8938.09	A	25.57	15.61
1992 Dec 10	8966.97	A	25.19	15.34
1993 Feb 05	9023.78	AnB	25.22	15.68
1993 Mar 21	9067.64	B	25.58	16.21
1993 Apr 09	9086.67	B	25.75	16.78
1993 May 18	9126.48	B→BnC	25.55	16.54
1993 Jul 25	9194.21	C	27.82	17.13
1993 Aug 26	9226.26	C	28.02	16.65
1994 Mar 04	9415.73	A	31.34	17.71
1994 Apr 11	9453.68	A	31.14	17.17
1994 May 07	9479.63	A→AnB	31.31	17.80
1994 Jun 25	9528.52	B	31.15	18.58
1994 Jul 06	9540.42	B	30.83	18.56
1994 Aug 18	9583.28	B	31.78	18.62
1994 Sep 08	9604.27	B	31.65	19.42
1994 Oct 10	9636.18	BnC	31.04	18.97
1994 Nov 07	9664.08	C	31.75	20.29
1994 Dec 08	9694.92	C	31.32	20.51
1995 Jun 23	9892.50	A	30.19	20.99
1995 Jul 08	9907.23	A	30.49	22.18
1995 Jul 21	9919.51	A	30.05	21.80
1995 Aug 07	9937.34	A	30.48	21.72
1995 Sep 01	9962.33	A	29.94	22.05
1995 Sep 09	9970.14	A→AnB	29.91	21.02

Table 2—Continued

Calendar Date	Day ^a	Array	Flux Density (mJy)	
			A Image	B Image
1995 Sep 15	9976.10	AnB	30.76	21.78
1995 Sep 23	9984.17	AnB	29.45	21.73
1995 Sep 30	9991.17	AnB	29.19	22.54
1995 Oct 10	10001.17	B	29.41	22.88
1995 Oct 27	10018.20	B	29.95	22.51
1995 Nov 09	10031.06	B	28.55	21.81
1995 Dec 26	10077.95	B	28.34	21.56
1996 Jan 26	10108.83	BnC	27.02	22.52
1996 Feb 05	10118.77	BnC	27.19	21.96
1996 Feb 26	10139.67	C	27.95	23.03
1996 Mar 04	10146.68	C	28.11	22.79
1996 Apr 05	10178.56	C	27.52	22.89
1996 Apr 25	10198.66	C	27.84	23.15
1996 Oct 19	10376.05	A	25.49	20.67
1996 Nov 10	10397.95	A	24.19	20.64
1996 Dec 26	10443.98	A	24.73	20.05
1997 Jan 10	10458.89	A	25.32	20.13
1997 Feb 26	10505.82	B	24.53	19.44
1997 Mar 19	10526.69	B	24.79	19.56
1997 Apr 10	10548.65	B	25.23	20.10
1997 May 11	10579.65	B	24.95	18.65
1997 Jun 22	10622.38	BnC	24.71	18.32
1997 Jul 11	10641.43	C	26.58	18.31
1997 Sep 22	10714.17	C	26.97	18.02

^aJulian Day – 2,440,000.0

Table 3. Results from PRHQ Statistic

Light Curve	Degrees of Freedom	Q	PRH χ^2		Time Delay (days)	Core Flux Ratio	c (mJy)	
			6 cm	4 cm			6 cm	4 cm
6 cm	291	165.5	344	...	459^{+12}_{-15}	$0.720^{+0.015}_{-0.014}$	$-1.04^{+0.58}_{-0.61}$...
6*cm	283	125.6	297	...	452^{+14}_{-15}	$0.731^{+0.014}_{-0.014}$	$-1.47^{+0.56}_{-0.62}$...
4 cm	113	15.7	...	111	397^{+12}_{-12}	$0.762^{+0.026}_{-0.031}$...	$-2.44^{+0.94}_{-0.77}$
6 cm & 4 cm	...	194.1	352	115	416^{+9}_{-8}	$0.744^{+0.011}_{-0.011}$	$-2.02^{+0.45}_{-0.49}$	$-1.78^{+0.37}_{-0.32}$
6*cm & 4 cm	...	148.6	302	113	409^{+9}_{-9}	$0.753^{+0.011}_{-0.012}$	$-2.35^{+0.45}_{-0.49}$	$-2.09^{+0.36}_{-0.33}$

*6 cm light curve with four points removed, see §4

Table 4. Results from Dispersion Statistic

Light Curve	Dispersion	Time Delay (days)
6 cm	0.608	430^{+23}_{-22}
6*cm	0.489	416^{+22}_{-24}
4 cm	0.259	383^{+15}_{-19}
6 cm & 4 cm	0.915	397^{+12}_{-15}
6*cm & 4 cm	0.764	395^{+13}_{-15}

*6 cm light curve with four points removed, see §4